

# Dynamic Properties of the Transient Network formed by Telechelic Ionomers Studied by Dynamic Light Scattering and Dynamic Mechanical Analysis

Ragnar Johannsson,<sup>†</sup> Christophe Chassenieux, Dominique Durand, and Taco Nicolai\*

Laboratoire de Physico Chimie Macromoléculaire, URA CNRS, Université du Maine, 72017 Le Mans Cedex, France

Pierre Vanhoorne and Robert Jérôme

Centre for Education and Research on Macromolecules, Institute of Chemistry B6, University of Liège, Sart Tilman, 4000 Liège, Belgium

Received June 28, 1995; Revised Manuscript Received September 18, 1995<sup>§</sup>

**ABSTRACT:** Solutions of  $\alpha,\omega$ -sodium sulfonatopolyisoprene ( $\alpha,\omega$  NaPIPS) in toluene are studied using static and dynamic light scattering and dynamic mechanical analysis. At concentrations above 4 g/L, which is well below the overlap concentration of the polymer chains ( $C^*$ ), a transient network is formed characterized by a plateau modulus at high frequencies and a relatively narrow viscoelastic relaxation time distribution. The intensity autocorrelation function of the transient network shows two relaxational modes: a relatively fast diffusional mode close to the co-operative diffusional mode of semidilute solutions of the unfunctionalized polymers and a slow broader mode which becomes independent of the scattering angle at a concentrations close to  $C^*$ . The relation between this slow mode and the viscoelastic relaxation is discussed. Both the slow mode and the viscoelastic relaxation processes have an Arrhenius temperature dependence with the same activation energy,  $E_a = 25$  kJ/mol.

## Introduction

Associative polymers contain small amounts of functional groups which associate in good solvents for the polymer backbone. Such systems are intensively studied both theoretically and experimentally because they have important industrial applications. Often the associating groups are randomly distributed along the polymer chain, which makes it difficult to understand their structure and dynamic properties. Telechelic polymers, i.e. polymers which contain only associating groups at the chain ends, can act as model systems for associative polymers in general. Two examples are  $\alpha,\omega$ -telechelic ionomers in apolar solvents<sup>1,2</sup> and triblock copolymers in solvents selective for the center block.<sup>3–7</sup> These systems show a strong increase of the viscosity at low concentrations where the viscosity of corresponding unfunctionalized polymer solutions is still close to that of the solvent. In some cases the viscosity diverges and the system behaves like a chemically cross-linked gel.

The dynamic properties of telechelic polymers have generally been studied by dynamic mechanical measurements and much less by dynamic light scattering. A systematic comparison of the dynamics as probed by these two techniques has as far as we know not yet been reported.

Here we present results from dynamic mechanical (DM) and dynamic light scattering (DLS) measurements on solutions of  $\alpha,\omega$ -sodium sulfonatopolyisoprene ( $\alpha,\omega$ -NaPIPS) with molar mass  $10^5$  g/mol in toluene at low concentrations. It will be shown that for concentrations above 4g/L a transient network is formed cross-linked by associating ionic groups. We will focus on the dynamic properties of the transient network as observed

by DLS and DM measurements. Due to the low refractive index increment of polyisoprene in toluene, it is not possible to measure accurately even more dilute solutions by DLS and thus to investigate the build-up of the network. However, we will discuss the main results of a recent DLS study on  $\alpha,\omega$ -lithium sulfonatopolystyrene with the same molar mass in toluene. We believe that the picture of the transient network build-up based on this study is valid also for the present system.

An estimate of the number of ionic groups per cross-link was obtained from fluorescence quenching (FQ) measurements.

## Experimental Section

**Materials.**  $\alpha,\omega$ -NaPIPS was synthesized by living anionic polymerization of isoprene as reported elsewhere.<sup>8</sup> The molar mass and polydispersity of the precursor polymer was determined by size exclusion chromatography (SEC):  $M_w = 8.9 \times 10^4$  g/mol,  $M_w/M_n = 1.4$ . Due to the high molar mass, the functionality could not be determined by titration. However, when the functionalized polymers are passed through the SEC columns, monotelechelic polymers (containing only one sulfonate group) are strongly retarded and telechelic polymers are irretrievably adsorbed to the column material. From this observation we conclude that the functionalization is almost complete for the system studied here, which is also expected from direct measurements on lower molar mass polymers synthesized by the same method.

**Dynamic Light Scattering.** DLS measurements were done using an ALV-5000 multibit, multitaue full digital correlator in combination with an Ar ion laser emitting vertically polarized light of wavelength 488 nm. In order to free the sample from spurious scatterers the polymer was first dissolved in spectra grade THF. In this solvent  $\alpha,\omega$ -NaPIPS does not associate and can be filtered through 0.2  $\mu$ m Anatope filters. The optical cleanliness after filtration was checked by DLS. The THF was subsequently removed by evaporation under vacuum after which spectra grade toluene was added to obtain the desired concentration. The samples were slowly rolled for 24 h to obtain homogeneous solutions. No effect of aging was observed for this system. All measurements were done at  $20 \pm 0.1$  °C unless otherwise specified.

<sup>†</sup> Present address: Technological Institute of Iceland, Keldnaholt IS-112 Reykjavik, Iceland.

<sup>§</sup> Abstract published in *Advance ACS Abstracts*, November 1, 1995.

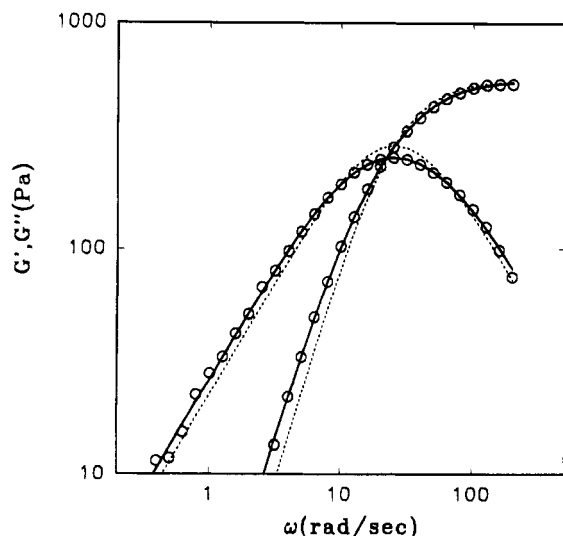


**Figure 1.** Frequency dependence of the loss and storage moduli for  $\alpha,\omega$ -NaPIPS at  $C = 26$  g/L. The solid lines represent the results of fits assuming a log-normal relaxation time distribution. The dashed line represents a single exponential relaxation.

**Dynamic Mechanical Analysis.** The frequency dependent shear modulus was measured on a Rheometrics RDA II apparatus with plate-plate geometry at room temperature. For one sample the temperature dependence was measured on a Haake RS 100 apparatus cone-plate geometry. The response was found to be linear for deformations less than 40%. All measurements were done in the linear response regime at a deformation of 5%.

**Fluorescence Quenching.** Fluorescence decays were determined on picosecond single-photon counting apparatus, using a mode-locked Nd:YAG laser (Spectra Physics, Model 3800) to synchronously pump a cavity dumped dye laser (Spectra Physics, Model 375) as an excitation source. The setup has been described.<sup>9</sup> (1-Pyrenebutyl)trimethylammonium bromide was used as a fluorescent probe. This probe self-quenches when two probe molecules encounter each other, so no further quencher is needed. The solutions were prepared as follows: a sufficient amount of  $6 \times 10^{-5}$  M solution of the probe in ethanol was placed in a flask and the ethanol evaporated by gently blowing nitrogen on the sample until dry. A polymer solution with  $C = 6.5$  g/L was then added and the solution was stirred for a few hours. The final concentration of the probe was determined by measuring the extinction at 346 nm. Prior to the measurements the solutions were degassed by bubbling of oxygen free nitrogen until no quenching from oxygen could be observed. A polymer free solution was used to check the solubility of the probe in toluene. No absorption was observed in this case, which shows that all the probe molecules are situated in the multiplets formed by associating ionic groups.

Care has to be taken not to have too high a probe concentration since the presence of the probes in the system can alter the aggregation number of the multiplet. For this reason, the average number of probes per multiplet was kept less than 1. Still, it is clear that for low aggregation numbers the presence of probes can have an effect on the system and the distribution of the probes between the multiplets might differ from a Poisson distribution.

## Results

**Dynamic Mechanical Data.** The frequency dependence of the shear modulus was measured for a number of concentrations between 6 and 35 g/L. At lower concentrations the viscoelastic response is too weak to determine accurately with the apparatus used in this study. In Figure 1 the loss and storage moduli are shown for  $C = 26$  g/L. We have analyzed the data by

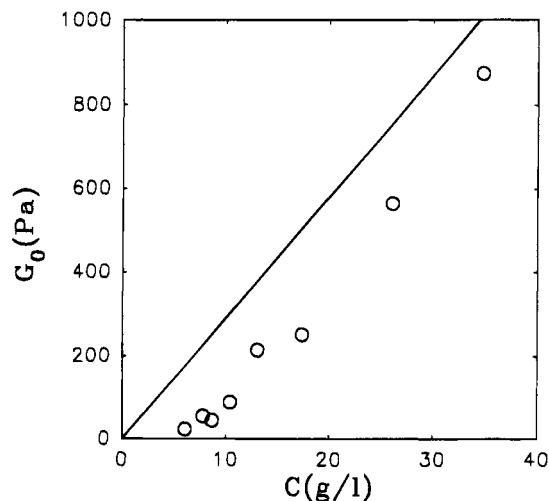


**Figure 2.** Concentration dependence of the gel modulus. The solid line represents the theoretical result for an ideal affine network.

assuming that the viscoelastic response can be described by a continuous sum of exponential decays:<sup>10</sup>

$$G'(\omega) = G_0 \int_0^\infty A(\tau) \frac{\omega^2 \tau^2}{1 + \omega^2 \tau^2} d\tau \quad (1)$$

$$G''(\omega) = G_0 \int_0^\infty A(\tau) \frac{\omega \tau}{1 + \omega^2 \tau^2} d\tau$$

where  $\omega$  is the angular frequency,  $A(\tau)$  is the amplitude of the decay with relaxation time  $\tau$ , and  $G_0$  is the high-frequency modulus. Experimentally, a simple log-normal distribution,

$$A(\log(\tau)) = \frac{1}{(2\pi)^{0.5} \sigma} \exp\left(-\frac{(\log(\tau) - \log(\tau_v))^2}{2\sigma^2}\right) \quad (2)$$

with

$$\log(\tau_v) = \int_0^\infty A(\tau) \log(\tau) d\tau$$

fits well to the data over the experimentally accessible frequency range as is shown by the solid lines through the data. Nonlinear least squares fits to  $G'$  and  $G''$  gave  $G_0 = 570 \pm 10$  Pa,  $\tau_v = (4.0 \pm 0.1) \times 10^{-2}$  s and  $\sigma = 0.23 \pm 0.01$ . The error bars result from the difference between the fit to  $G'$  and  $G''$ . For comparison we have also plotted as dotted lines in Figure 1 the results of a single decay with the same  $G_0$  and  $\tau_v$ . Similar almost single exponential decays have been observed for different telechelic ionomers<sup>1,2</sup> and for triblock copolymers.<sup>3</sup>

The width of the distribution,  $\sigma$ , is found to be independent of the concentration. The concentration dependence of the characteristic relaxation time,  $\tau_v$ , and the high-frequency modulus are shown in Figures 2 and 3. While  $G_0$  increases strongly with increasing concentration above  $C \approx 8$  g/L,  $\tau_v$  does not vary with  $C$  in a systematic way. We believe that the scatter in the values of  $\tau_v$  is not due to inaccuracies of the measurements, but is caused by the presence of different amounts of traces of polar substances like water in the solvent (see the Discussion section).

Unfunctionalized polyisoprene of this molar mass has a purely viscous behaviour at the concentrations and angular frequencies covered in this study.

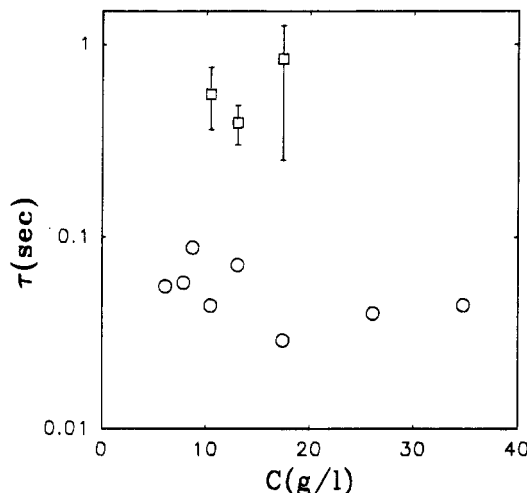


**Figure 3.** Concentration dependence of the viscoelastic relaxation time (circles) and the  $q$ -independent relaxation time observed by dynamic light scattering (squares). The error bars indicate the spread of the latter at different scattering wave vectors.

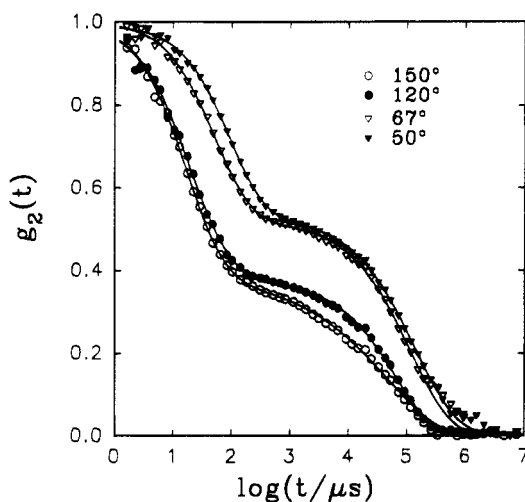


**Figure 4.** Normalized intensity autocorrelation functions measured for  $\alpha,\omega$ -NaPIPS ( $C = 10$  g/L) at different angles of observation indicated in the figure. For clarity, only one in four points is shown. The solid lines represent the results of fits to eqs 3 and 4.

**Dynamic Light Scattering.** Dynamic light scattering experiments were done for a number of polymer concentrations above  $C = 4$  g/L. The very low contrast between polyisoprene and toluene precludes accurate measurements on lower concentrations. For all concentrations we can distinguish at least two relaxational processes: a relatively fast mode which increases with the square of the scattering wave vector,  $q$ , and a slower mode which is  $q$ -independent for  $C > 9$  g/L [ $q = (4\pi n/\lambda) \sin(\Theta/2)$ ], with  $n$  being the refractive index,  $\lambda$  the wavelength, and  $\Theta$  the angle of observation]. This is shown in Figure 4, where the normalized intensity autocorrelation function,  $g_2(t)$ , is plotted for four different values of  $q$  of the sample with  $C = 10$  g/L. The data were analyzed assuming that the electric field autocorrelation function can be described by a continuous sum of exponential decays:

$$g_2(t) = \left( \int_0^\infty A(\tau) \exp\left(-\frac{t}{\tau}\right) d\tau \right)^2 \quad (3)$$

where we have used the so-called Siegert relation to

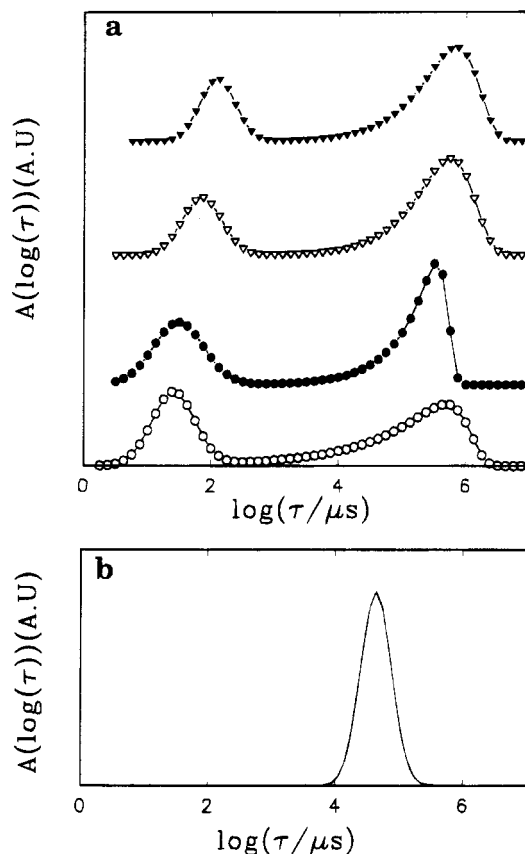


**Figure 5.** Relaxation time distributions for  $\alpha,\omega$ -NaPIPS at  $C = 10$  g/L obtained from dynamic light scattering and dynamic mechanical spectroscopy. (a) obtained from the correlograms shown in Figure 4 and (b) obtained from the frequency dependence of the shear modulus shown in Figure 1.

relate the electric field autocorrelation function to the intensity autocorrelation function.<sup>11</sup> A number of computer routines fit  $g_2(t)$  to eq 3 without assuming a specific shape for  $A(\tau)$ .<sup>12</sup> However, broad distributions tend to be represented by a multiple peaked distribution, due to the nonrandom noise on the correlation function.<sup>13</sup> Therefore we have chosen  $A(\tau)$  as the sum of a log-normal distribution to represent the fast process and a so-called generalized exponential (GEX) to represent the slower process:

$$A(\log(\tau)) = \frac{A_1}{(2\pi)^{0.5} \sigma} \exp\left(-\frac{(\log(\tau) - \log(\tau_1))^2}{2\sigma^2}\right) + \frac{A_2}{k} \tau^p \exp[-(\tau/\tau_2)^s] \quad (4)$$

where  $k$  is a normalization constant such that

$$\int_0^\infty \frac{1}{k} \tau^p \exp[-(\tau/\tau_2)^s] d(\log(\tau)) = 1$$

$s$  and  $p$  are parameters which allow a wide shape variation of the GEX distribution. This type of analysis was used earlier in the study of semidilute polymer solutions in  $\Theta$  solvents.<sup>14</sup> The results of nonlinear least squares fits to eqs 3 and 4 are shown as solid lines in Figure 4. The corresponding relaxation time distributions are shown in Figure 5a. For comparison we show in Figure 5b the relaxation time distribution obtained from the shear modulus measurement on the same sample.

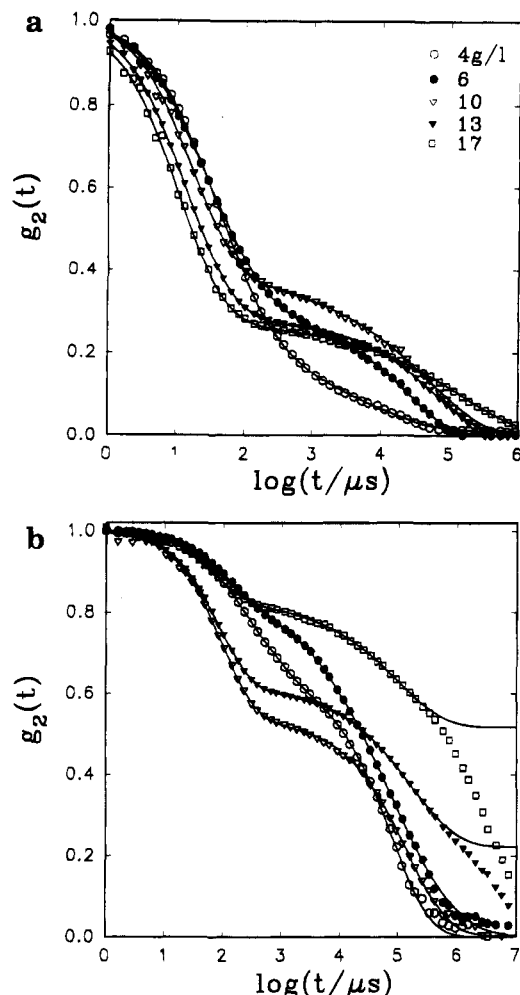


**Figure 6.** Normalized intensity autocorrelation functions measured for  $\alpha,\omega$ -NaPIPs at different concentrations indicated in the figure. For clarity, only one in four points is shown. The solid lines represent the results of fits to eqs 3 and 4: (a) Data obtained for an angle of observation  $150^\circ$ , (b) Data obtained for an angle of observation  $50^\circ$ . For the highest two concentrations, the data were fit for  $t < 2 \times 10^5 \mu\text{s}$  and a floating base line was included.

At concentrations lower than 9 g/L the peak position of the slow mode is not  $q$ -independent, but increases with increasing  $q$  although more slowly than a  $q^2$ -dependence. At concentrations larger than 10 g/L a third very slow and ill-defined relaxational process can be observed. The relative amplitude of this relaxational process is strongly  $q$ - and concentration-dependent. At small scattering wave vectors the contribution which gives rise to this third mode dominates the total scattering. The higher the concentration the more important the contribution of this third relaxational process is even at larger values of  $q$ . We attribute this third process to large scale inhomogeneities in these increasingly viscous samples. In Figure 6 the correlation functions are shown at different concentrations at two angles of observation. At the highest two concentrations the contribution of the third mode is clearly visible. The solid lines through the data represent linear least squares fits to eqs 3 and 4. If the contribution of the third mode could not be neglected, we cut the correlation function at a shorter time and treated it as a floating base line in the fit. In practice the  $q$ -independent mode can only be determined over a very limited range of concentrations. In Figure 3 we have plotted the peak position of the  $q$ -independent mode,  $\tau_d$ .

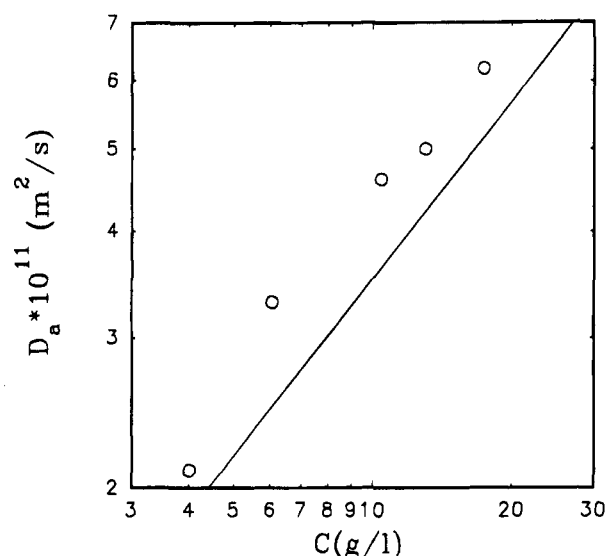


**Figure 7.** Concentration dependence of the apparent diffusion coefficient. The solid line represents the concentration dependence of the co-operative diffusion coefficient of semidilute solutions of linear polyisoprene in good solvents.

The error bars indicate the largest and smallest value measured in the  $q$ -range  $(1.6\text{--}3.1) \times 10^7 \text{ m}^{-1}$ . We stress that although the error bars are large, especially at the highest concentration, there is no systematic variation with  $q$ . A comparison with  $\tau_v$  shows that the characteristic relaxation time measured by DLS is almost a factor of 10 larger than the relaxation time obtained from the shear modulus. In addition, Figure 5 shows that the relaxation time distribution measured by DLS is broader than the one obtained from the shear modulus.

The fast relaxation is in all cases  $q^2$ -dependent so that we can calculate an apparent diffusion coefficient,  $D_a$ , from the relaxation rate of this mode:  $\Gamma = D_a q^2$ . In Figure 7 the concentration dependence of  $D_a$  is compared with the co-operative diffusion coefficient of semidilute solutions of linear and branched polyisoprene in another good solvent<sup>15</sup> after correction for the difference in solvent viscosity. The small difference indicates that the fast mode is due to co-operative diffusion which is only weakly modified by the presence of associative groups on the chain ends.

The temperature dependence was measured between  $5.0$  and  $77^\circ\text{C}$  for  $C = 10 \text{ g/L}$ . Over this temperature range the second mode is  $q$ -independent. At temperatures below  $-5^\circ\text{C}$  the solutions cloud, which indicates a phase separation. Correlation functions obtained at various temperatures are shown in Figure 8 where the time axis has been corrected for the variation of the solvent viscosity. After correction for the solvent viscosity the fast mode is independent of the temperature, while the slow mode has an Arrhenius temperature dependence:  $\tau_d \propto \exp(E_a/kT)$ , with  $E_a = 25 \pm 2 \text{ kJ/mol}$  (see Figure 9). The temperature dependence of  $\tau_v$  could only be measured over a small temperature range and is included in Figure 9 for comparison. It is clear that over the limited temperature range investigated the temperature dependence is the same.

**Fluorescence Quenching.** Figure 10 shows the self-quenched decay of the fluorescence of (1-pyrenebutyl)trimethylammonium bromide in a solution of  $\alpha,\omega$ -NaPIPs in toluene. A fast decay due to self-quenching in multiplets containing two or more probes is followed by a single exponential decay of unquenched probes.

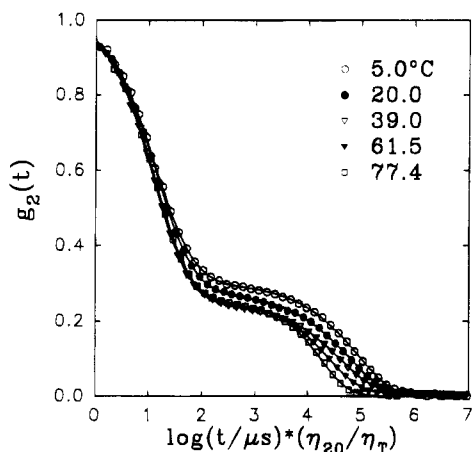


**Figure 8.** Normalized intensity autocorrelation functions measured for  $\alpha,\omega$ -NaPIPS ( $C = 10$  g/L,  $\theta = 150^\circ$ ) at different temperatures indicated in the figure.

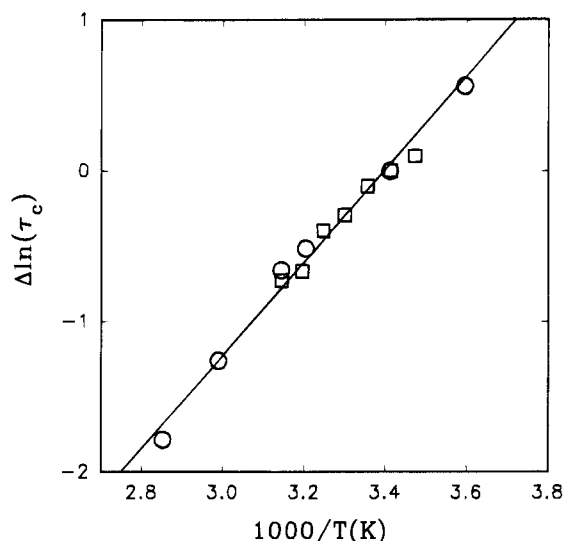


**Figure 9.** Arrhenius plot of the relaxation time of the  $q$ -independent mode obtained from DLS of  $\alpha,\omega$ -NaPIPS in toluene ( $C = 10$  g/L) (circles). The solid line represents the result of a linear least squares fit to the data. The temperature dependence of the viscoelastic relaxation is shown for comparison (squares). The data are normalized to the value at  $20^\circ\text{C}$ .

It has been shown by Infelta et al.<sup>16</sup> that the fluorescence decay curves from quenching in micelles can be described as

$$\ln(F(t)/F(0)) = -t/\tau_0 + m(\exp(-k_q t) - 1) \quad (5)$$

if no migration between the micelles takes place. Here  $F(0)$  is the fluorescence intensity at  $t = 0$ ,  $m$  is the average number of quenchers per micelle,  $\tau_0$  is the lifetime of the unquenched probes, and  $k_q$  is the first-order quenching rate constant inside the micelle. The solid line in Figure 10 represents a nonlinear least squares fit to eq 5, which clearly gives a good representation of the data. Since the molar concentration of ionic end groups,  $[S]$ , and probes,  $[Q]$ , is known, the number of ionic groups per multiplet,  $n_m$ , can be calculated from  $m$  as follows:

$$n_m = m[S]/[Q] \quad (6)$$

Measurements at two different probe concentrations give  $n_m = 7.5$  for  $[Q]/[S] = 0.075$  and  $n_m = 8.2$  for  $[Q]/[S]$

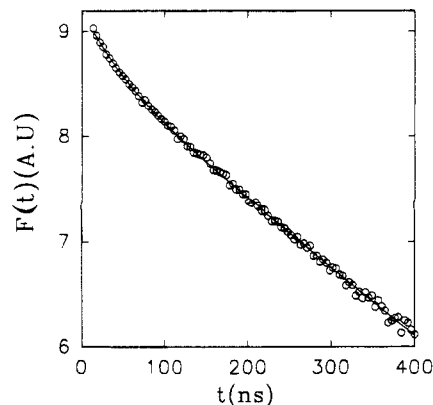


**Figure 10.** Self-quenched fluorescence decay of (1-pyrenebutyl)trimethylammonium bromide in a solution of  $\alpha,\omega$ -NaPIPS in toluene with  $C = 0.65$  g/L. The solid line represents a nonlinear least squares fit to eq 5.

$= 0.035$ . However, for reasons outlined in the Experimental Section the fluorescence quenching technique could give biased results for small aggregation numbers, so we consider this value of  $n_m$  only as a rough estimate.

## Discussion

It is now generally accepted that the ionic groups of telechelic ionomers associate into small multiplets in apolar solvents due to dipolar interactions.<sup>1,2</sup> The detailed structure of these multiplets depends on the dielectric constant of the solvent, the type of ionic group and counterion and the size and structure of the polymer. Temperature and presence of traces of polar substances also have an influence. As yet, no theory can predict the number of ionic groups per multiplet for a given system. Light scattering measurements on monotelechelic ionomers, which contain a single ionic group, show that there is a preferred configuration of the multiplet and that the variation around an average value of  $n_m$  is narrow.<sup>17–20</sup> From these measurements it is also clear both that the critical association concentration, CAC, is very low and that  $n_m$  is not very sensitive to the concentration at least at low concentrations. Small angle X-ray (SAXS) measurements show that also at high concentrations  $n_m$  remains constant both for telechelic and monotelechelic ionomers.<sup>21,22</sup>

The small refractive index increment of polyisoprene in toluene precludes accurate light scattering measurements at very low concentrations. Recently, a detailed light scattering study was conducted<sup>20</sup> on  $\omega$ - and  $\alpha,\omega$ -lithium sulfonatopolystyrene (LiPSS) with almost the same molar mass in toluene covering also the very dilute regime. We will give the main results here, because we believe that they are not system specific and will help to explain the  $\alpha,\omega$ -NaPIPS system.

Above a CAC of  $0.2$  g/L  $\omega$ -LiPSS forms aggregates with an aggregation number 4 independent of the concentration. The aggregates behave as starlike polymers with four arms up to the highest concentration investigated ( $C = 66$  g/L), which is above the overlap concentration,  $C^*$ , for the unaggregated polymer. We define  $C^*$  as  $(3M)/(4\pi N_a R_g^3)$  with  $N_a$  being Avogadro's number and  $R_g$  the radius of gyration. For the polystyrene (PS) with  $M = 10^5$  g/mol,  $C^* = 27$  g/L, while for the Polyisoprene (PIP) with the same molar mass,  $C^* = 11$  g/L, where we have used the relation between the molar mass and the radius of gyration in good solvents for PS given in ref 23 and for PIP given in ref 24. For  $\alpha,\omega$ -LiPSS the CAC is difficult to establish accurately,

but is less than 0.01 g/L. The size distribution of the aggregates was determined by DLS. At the lowest concentrations the size distribution is similar to that of the precursor polymer and the aggregation number is again about 4. As the concentration increases the average aggregation number increases and the size distribution broadens. The increase in size cannot be explained by an increase of  $n_m$ , but is due to interconnection of an increasing number of multiplets. If we suppose that at the lowest concentrations the aggregates contain only one multiplet, the number of ionic groups per multiplet will be between four and eight depending on whether loop formation occurs.

At concentrations above 5 g/L, DLS gives two relaxational modes like we have seen for  $\alpha,\omega$ -NaPIS. Like in the case of  $\alpha,\omega$ -NaPIS the second mode has initially some  $q$ -dependence, but becomes  $q$ -independent at higher concentrations. Very slow relaxations are observed also in the case of  $\alpha,\omega$ -LiPSS at high concentrations and small values of  $q$ . At 5 g/L the correlation function can be analyzed either in terms of a single broad mode or two modes.

The light scattering measurements on  $\alpha,\omega$ -LiPSS show that the multiplets interconnect into larger aggregates already at concentrations much below the overlap concentration of single multiplets. This aggregation process can be understood in terms of an open association model. At a concentration close to 5 g/L, a space-filling transient network is formed and a gel modulus is observed at frequencies faster than the lifetime of an ionic group in the multiplet. The gel modulus increases with increasing concentration as more and more clusters become part of the network and the number of loops in the network reduces. The fact that the viscoelastic relaxation time is independent of the concentration indicates that the structure of the multiplets does not change much with increasing concentration.

If we assume that an affine network is formed, the gel modulus can be related to the number of elastically active chains,  $\nu$ , in mole per unit of volume:<sup>25</sup>

$$G_0 = \nu RT \quad (7)$$

with  $R$  being the gas constant. In Figure 2 we compare  $G_0$  calculated using eq 7 and assuming that all the chains contribute to the gel modulus of  $\alpha,\omega$ -NaPIS. It is clear that at highest concentrations almost all chains are indeed elastically active. At higher concentrations,  $G_0$  is expected to increase even more when topological entanglements become important.

Annabale has presented a detailed model to explain the increase in  $G_0$  with increasing concentration assuming that all clusters are part of the transient network.<sup>3</sup> The model involves a statistical description of the number of loops, free ends, and superchains, which are chains connected by a bifunctional multiplet. This model describes qualitatively well the concentration dependence of  $G_0$ , but for a more quantitative description we need to know both  $n_m$  and the shape of the distribution around the average value. However, if  $n_m$  is much larger than 3, as was shown by FQ, the contribution of loops, free ends, and superchains becomes negligible at higher concentrations and  $G_0$  only depends on the number of chains in the solution regardless the strength of the interactions between the ionic groups. On the other hand, the relaxation time and consequently the viscosity are strongly dependent on the strength of the interactions and therefore very

sensitive to traces of polar substances in the solution. The presence of traces of for example water could explain the scatter in the measured value of  $\tau_v$ .

Often the critical concentration for gelation,  $C_{gel}$ , is taken as the concentration where the viscosity of the system diverges. Of course, as  $\eta \propto G_0\tau_v$ , true divergence only occurs if  $\tau_v = \infty$ , but as long as  $\tau_v$  is not too small, the viscosity increases sharply when the transient network is formed. Thus, the concentration where the viscosity appears to diverge gives a good, but maybe slightly overestimated, value of  $C_{gel}$ . If  $\tau_v$  is very large, it will take too long to equilibrate the system, so the structure of the network and therefore its mechanical properties depend on the history of the sample.

As mentioned, at a concentration close to  $C_{gel}$  two relaxational modes become clearly distinguishable by DLS. The diffusion constant characterizing the fast diffusional mode is close to the co-operative diffusion coefficient in semidilute solutions of the nonfunctionalized polymers in good solvents. The slow  $q$ -independent mode at higher concentrations is reminiscent of semidilute polymer solutions in poor solvents.<sup>14</sup> For these systems a clear relation between this relaxation and the viscoelastic relaxation has been established experimentally. A number of people have given theoretical expressions of the correlation function due to concentration fluctuations which include the viscoelastic relaxation for polymer solutions above the overlap concentration.<sup>26-29</sup> The general expression reads

$$\hat{g}(s) = \frac{\tau_c + \frac{\hat{M}(s)}{K_{os}}}{s\left(\tau_c + \frac{\hat{M}(s)}{K_{os}}\right) + 1} \quad (8)$$

where  $\hat{g}(s) = \int g_1(t) \exp(-st) dt$  is the Laplace transform of the electric field autocorrelation function,  $\hat{M}(s)$  is the Laplace transform of the time-dependent longitudinal elastic modulus,  $M(t)$ , and  $K_{os} = C(d\pi/dC)$  is the osmotic modulus. If  $M(t) \ll K_{os}$ , the correlation function is single exponential with a  $q^2$ -dependent relaxation time  $\tau_c = (D_c q^2)^{-1}$ . The co-operative diffusion coefficient in the laboratory coordinate system is related to the osmotic modulus and the friction coefficient between the polymers and the solvent,  $f$ :  $D_c = (1 - \varphi)^2 K_{os} / f$ ,<sup>11,30</sup> with  $\varphi$  being the volume fraction of the polymers. If the elastic modulus is not negligible,  $g_1(t)$  is still single exponential if  $\tau_c$  is much larger than the largest viscoelastic relaxation time. However, if the diffusional relaxation is faster than the viscoelastic relaxation, slow relaxational modes are expected with a relative amplitude determined by the relative strength of the elastic modulus compared to the osmotic modulus. Slow modes are generally not observed in semidilute polymer solution in good solvents because  $K_{os} \gg M(t)$ , even though the viscoelastic relaxation is slower than the co-operative diffusion.

The general expression, eq 8, is much simplified if  $M(t)$  is characterized by a single relaxation time much larger than  $\tau_c$ . In this case it is possible to give an analytical expression of  $g_1(t)$ :

$$g_1(t) = A_f e^{-D_c q^2 t} + A_s e^{-t/\tau_s} \quad (9)$$

The relative amplitude of the slow mode depends on the relative strength of the longitudinal gel modulus,  $M_0$ ,

but is independent of  $q$  as long as  $\tau_c \ll \tau_v$ :  $A_0/A_s = K_{os}/M_0$ . The co-operative diffusion coefficient increases due to the contribution of the gel modulus:  $D_c = (1 - \varphi)^2 \cdot (K_{os} + M_0)/f$ . The slow relaxation is  $q$ -independent with a relaxation time related to the viscoelastic relaxation time:  $\tau_s = \tau_v(M_0/K_{os})$ .

For the system studied here the viscoelastic relaxation is characterized by a narrow distribution of relaxation times much slower than the co-operative diffusion. A slow  $q$ -independent relaxational mode is therefore expected if  $K_{os}$  is not much larger than  $M_0$ .  $M_0$  contains contributions of the bulk gel modulus and the shear gel modulus:  $M_0 = K_0 + 4G_0/3$ . For covalent dilute gels the bulk gel modulus does not relax and modifies the osmotic modulus.<sup>31</sup> We are only able to measure  $G_0$  values that are on the same order of magnitude as the osmotic modulus of semidilute polyisoprene solutions in good solvents. The fact that the relative contributions of the two modes to  $g_1(t)$  are close is consistent with the theory, provided  $K_0$  is not much larger than  $G_0$ , although we observe a weak  $q$ -dependence of the relative amplitude. The main inconsistency with the theory is, however, that  $\tau_s$  is almost a factor 10 larger than  $\tau_v$ . This would imply that  $M_0$  is a factor 10 larger than  $K_{os}$ , but in that case the slow mode should be dominant and  $D_c$  should be much larger than the corresponding value for semidilute solutions of nonfunctionalized polymers. In addition, the relaxation time distribution obtained from DLS is broader than the viscoelastic relaxation time distribution.

An alternative explanation would be that the slow relaxation is due to diffusion and/or restructuring of small scale inhomogeneities. If the diffusion is faster than the lifetime of the multiplets, the break-up of the multiplet becomes the limiting time step for the diffusion of such inhomogeneities and the relaxation time will be  $q$ -independent. If the relaxation is due to restructuring, a  $q$ -independent relaxation is also expected. In both cases the characteristic relaxation time would be larger than  $\tau_v$  and with a broader distribution as more than one escape of an ionic group from a multiplet could be involved in such a relaxation.

Whatever the physical origin of the slow  $q$ -independent relaxation, it is most likely related to the viscoelastic relaxation, as is evidenced by the similar Arrhenius temperature dependence.

## Summary

$\alpha,\omega$ -NaPIPS of molar mass  $10^5$  g/mol forms transient networks in toluene at concentrations larger than 4 g/L. The shear modulus is characterized by a narrow relaxation time distribution with a concentration-independent relaxation time. The gel modulus increases strongly for concentrations larger than about 8 g/L and is determined by the concentration of polymer chains at high concentrations.

Autocorrelation functions determined by dynamic light scattering are characterized by two relaxational processes: a faster  $q^2$ -dependent mode and a slower mode which becomes  $q$ -independent at  $C > 9$  g/L. The fast mode is close to the co-operative diffusional mode observed for semidilute solutions of polyisoprene in good solvents. The slow mode has an Arrhenius temperature

dependence and is probably related to the viscoelastic relaxation. A third very slow and ill-defined relaxation process is observed at high concentrations and small scattering wave vectors. This mode is attributed to large scale inhomogeneities in the increasingly viscous samples.

**Acknowledgment.** We thank Per Hansson and Mats Almgren for their assistance with the fluorescence-quenching experiments.

## References and Notes

- (1) Jérôme, R. In *Telechelic Polymers: Synthesis and Applications*, Goethals, E. J., Ed.; CRC Press: Boca Raton, FL, 1989; Chapter 11.
- (2) Butler, G. B.; O'Driscoll, K. F.; Wilkes, G. L. *J. Macromol. Sci., Rev. Macromol. Chem. Phys.* **1988**, C28 (1).
- (3) Annable, T.; Buscall, R.; Ettelai, R.; Whittlestone, D. *J. Rheol.* **1993**, 37, 695. Annable, T.; Buscall, R.; Ettelaie, R.; Shepherd, P.; Whittlestone, D. *Langmuir* **1994**, 10, 1060.
- (4) Raspaud, E.; Lairez, D.; Adam, M.; Carton, J.-P. *Macromolecules* **1995**, 28, 927.
- (5) Mortensen, K.; Brown, W.; Jørgensen, E. *Macromolecules* **1994**, 27, 5654.
- (6) Yekta, A.; Xu, B.; Duhamel, J.; Adiwidjaja, H.; Winnik, M. A. *Macromolecules* **1995**, 28, 956.
- (7) Nyström, B.; Walderhaug, H.; Hansen, F. K. *J. Phys. Chem.* **1993**, 97, 7743.
- (8) Boiteux, G.; Foucart, M.; Jérôme, R. *Polymer* **1992**, 33, 4242.
- (9) Almgren, M.; Hansson, P.; Mukthar, E.; van Stam, J. *Langmuir* **1992**, 8, 2405.
- (10) Ferry, J. D. *Viscoelastic Properties of Polymers*, 2nd ed.; Wiley: New York, 1970.
- (11) Berne, B.; Pecora, R. *Dynamic Light Scattering*; Wiley: New York, 1976.
- (12) Stepanek, P. In *Dynamic Light Scattering*; Brown, W., Ed.; Oxford University Press: Oxford, 1993; Chapter 4.
- (13) Peters, R. In *Dynamic Light Scattering*; Brown, W., Ed.; Oxford University Press: Oxford, 1993; Chapter 3.
- (14) Nicolai, T.; Brown, W.; Hvidt, S.; Heller, K. *Macromolecules* **1990**, 23, 5088.
- (15) Adam, M.; Fetters, L. J.; Graessley, W. W.; Witten, T. A. *Macromolecules* **1991**, 24, 2434.
- (16) Infelta, P. P.; Grätzel, M.; Thomas, J. K. *J. Phys. Chem.* **1974**, 78, 190. Infelta, P. P. *Chem. Phys. Lett.* **1979**, 61, 88.
- (17) Vanhoorne, P. Ph.D. dissertation, University of Liège, 1994.
- (18) Pispas, S.; Hadjichristidis, N.; Mays, J. W. *Macromolecules* **1994**, 27, 6307.
- (19) Möller, M.; Mühleisen, E.; Omeis, J. In *Physical Networks: Polymers and Gels*; Burchard, W., Ross-Murphy, S. B., Eds.; Elsevier Applied Science: London, 1990; Chapter 4.
- (20) Chassenieux, C.; Johannsson, R.; Nicolai, T.; Durand, D.; Vanhoorne, P.; Jérôme, R. *Colloids Surf.*, in press.
- (21) Vanhoorne, P.; Maus, C.; Van den Bossche, G.; Fontaine, F.; Sobry, R.; Jérôme, R.; Stamm, M. *J. Phys. IV* **1993**, 3(C8), 63.
- (22) Vanhoorne, P.; Van den Bossche, G.; Fontaine, F.; Sobry, R.; Jérôme, R.; Stamm, M. *Macromolecules* **1994**, 27, 838.
- (23) Miyaki, Y.; Einaga, Y.; Fujita, H. *Macromolecules* **1978**, 11, 1180.
- (24) Tsunashima, Y.; Hirata, M.; Nemoto, N.; Kurata, M. *Macromolecules* **1988**, 21, 1107.
- (25) Mark, J. E.; Ergan, B. *Rubberlike Elasticity a Molecular Primer*; Wiley & Sons: New York, 1988.
- (26) Doi, M.; Onuki, A. *J. Phys. II Fr.* **1992**, 2, 1631.
- (27) Genz, U. *Macromolecules* **1994**, 27, 5691.
- (28) Akcasu, Z.; Klein, R.; Wang, C. H. *Macromolecules* **1994**, 27, 2736.
- (29) Semenov, A. N. *Physica A* **1990**, 166, 263.
- (30) Vink, H. J. *J. Chem. Soc. Faraday Trans.* **1985**, 81, 1725.
- (31) Geissler, E. In *Dynamic Light Scattering*; Brown, W., Ed.; Oxford University Press: Oxford, 1993; Chapter 11.

MA9509164